# Density Functional Study of the Interactions between Dihydrogen and Pd$_n$ ($n = 1-4$) Clusters

**Irena Efremenko,\* Ernst D. German, and Moshe Sheintuch**

*Wolfson Department of Chemical Engineering, Technion−Israel Institute of Technology, Haifa 32000, Israel*

*Received: March 9, 2000; In Final Form: May 16, 2000*

The dihydrogen interactions with Pd$_n$ ($n = 1-4$) clusters was investigated using hybrid density functional Becke3LYP method and two ECP basis sets. The local minima configurations for a number of H$_2$ molecule approach modes toward Pd$_n$ clusters are presented. Some of these states may be interpreted as a physical adsorption and others as dissociative interaction of the H$_2$ molecule with the palladium cluster. Both geometric and energetic characteristics of weakly bonded pre-dissociated complexes on Pd$_{3-4}$ clusters are very close to those on a bulk Pd (111) surface, while the stable states with dissociated hydrogen molecules show significant differences. In contrast to the bulk surface, 2-fold coordination positions exhibit slightly higher stability of hydrogen bonding in Pd$_3$ and Pd$_4$ clusters than 3-fold ones. The binding energy is significantly higher for small clusters than for the bulk surface. The Pd$_2$ cluster was found to be the most active toward hydrogen capture in accordance with the experimental results.

## Introduction

Small palladium clusters are promising candidates for catalytic applications, particularly, in reactions of hydrogenation and dehydrogenation.[1] The hydrogen activation is an important if not the key stage determining the mechanism and corresponding direction, activity, and selectivity of the reactions. Thus, theoretical investigation of hydrogen activation by palladium clusters plays an important role in modeling of processes which are catalyzed by highly dispersed particles, and may shed light on the understanding of catalytic reactions on bulk metal surfaces.

Experimentally, it was shown that hydrogen interaction with small palladium clusters is a strong function of cluster size.[2] To our knowledge, high-level calculations on Pd$_n$/H$_2$ systems were restricted to $n = 1-3$.[3−11] Interaction between Pd$_4$ and H$_2$ was investigated only for one planar configuration of metal atoms.[12] In most of these works palladium clusters served as models of bulk surfaces and their geometry was fixed at the *fcc* palladium crystalline lattice. The structure of real-life small palladium clusters was shown to differ significantly as compared to the bulk configuration,[13,14] and an adsorbent-induced relaxation of cluster geometry is expected to be quite pronounced. Full optimization of the geometry was done for Pd$_n$−H$_2$ systems with $n = 2,3$ in the DFT studies;[9,10] however, only a few approach modes and corresponding stationary states were considered. Some of reaction paths and local minima, especially those associated with weak interactions, which are of special importance in catalytic reactions, have received little attention. Thus, future study of Pd−H$_2$ interactions using the relevant model of small palladium clusters with optimized geometry seems to be important for the understanding of cluster catalyst performance.

In this paper we present the analysis of the local minima along several directions of a hydrogen molecule approach to Pd$_n$ ($n = 1-4$) clusters including weakly bonded states. Examination of distinct approach directions of reagents, i.e., cross-sections of many-dimensional potential energy surfaces (PES), and of corresponding stationary states is used extensively for studying reactions with complicated structure of PES since such approximation allows one to obtain detailed information on special regions of PES cross-section. The results of our calculations are compared with the corresponding literature data in order to reveal an influence of cluster relaxation on Pd$_n$−H$_2$ interaction. Size dependencies of hydrogen binding energy for different adsorption states are presented in comparison with corresponding literature results for the bulk Pd (111) surface.

## Computational Details

The calculations have been carried out using DFT method as it is implemented in *Gaussian94*.[15] We adopted a B3LYP functional that combines Becke's three-parameter hybrid exchange functional[16] with the correlation functional by Lee et al.[17] For hydrogen, Dunning's cc-pVDZ basis set was used.[18] Two effective core potential (ECP) basis sets[19] were employed for Pd atoms. The first one was the standard Los Alamos National Laboratory set of double-$\zeta$ type (LANL2DZ) with 28 core electrons been replaced by LANL2 ECP and 4s4p4d5s valence electrons been treated explicitly by the contraction scheme (8s/6p/4d)/[341/321/31] (basis I). The B3LYP/LANL2DZ combination was shown recently[20] to yield good results for small Pd clusters. The second basis set (basis II) was one of LANL1DZ[19] type, in which the ECP LANL1 replaces 36 core electrons with contraction scheme (3s3p4d)/[2s1p1d][21] for the valence 4d and 5s,p orbitals as opposed to the standard LANL1DZ contraction (3s3p4d)/[2s2p2d]. Basis II is more economic than both LANL1DZ and LANL2DZ and better describes the dissociation energies of Pd$_2$ and Pd−H dimers than the standard LANL1DZ basis (Table 1). Comparison of the considered basis sets presented in Table 1 shows as well that basis I, in contrast to smaller ones, provides the triplet ground state for Pd$_2$ (as well as for other small palladium clusters). The effect of basis set superposition error (BSSE) was calculated using the classical counterpoise correction method[27]

* Corresponding author. Fax: 972-4-8230476. E-mail: chrirena@tx.technion.ac.il.
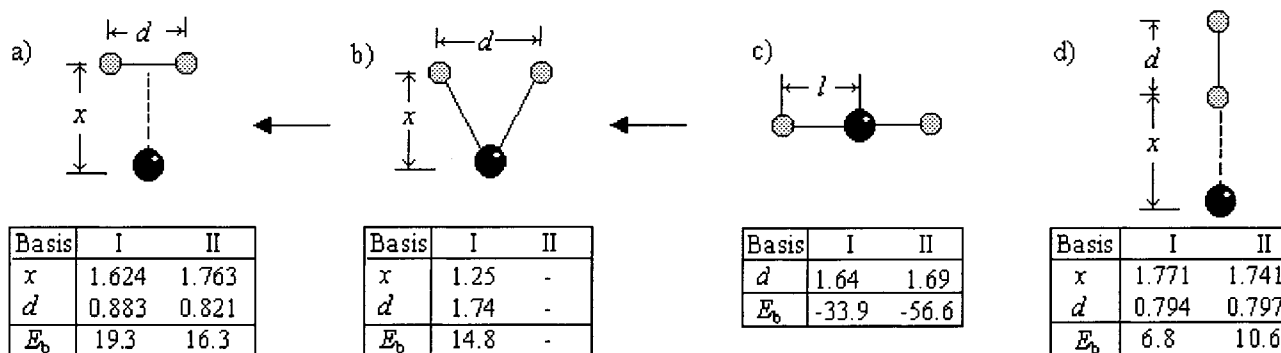
**Figure 1.** Geometries (Å) and corresponding binding energies (kcal/mol) of stationary states in the Pd−$H_2$ system.

**TABLE 1: Equilibrium Bond Lengths ($r_{eq}$, Å), Dissociation Energies ($D$, kcal/mol), and Harmonic Vibrational Frequencies ($\omega$, cm$^{-1}$) for PdH and $Pd_2$ Molecules**

| basis set for Pd | | | basis I | basis II | LANL1DZ | experiment |
|---|---|---|---|---|---|---|
| | $R_{eq}$ | | 1.540 | 1.578 | 1.577 | 1.534;[a] 1.529[b] |
| Pd−H | $D^d$ | | 54.3 | 40.4 | 30.4 | 55± 6[c] |
| | $\omega$ | | 2037 | 1750 | 1762 | 2083[e] |
| | $R_{eq}$ | singlet | 2.762 | 2.743 | 2.840 | |
| | | triplet | 2.526 | 2.426 | 2.770 | |
| Pd−Pd | $D^f$ | singlet | 11.2 | 6.1 | 5.5 | 17 ± 3; 26 ± 5[g] |
| | | triplet | 19.1 | 0.8 | −40.3 | |
| | $\omega$ | singlet | 133.9 | 111.4 | 89.5 | 200 ± 15[h] |
| | | triplet | 206.6 | 194.7 | 117.7 | |

[a] Ref 22. [b] Ref 23. [c] Ref 24. [d] $D = E(H) + E(Pd) − E(PdH)$ with zero point and BSSE corrections (see text for details). [e] Estimation using the vibration frequency of Pd−D bond from ref 22. [f] $D = 2E(Pd) − E(Pd_2)$. [g] Ref 25. [h] Ref 26.

**TABLE 2: Experimental and Calculated Characteristics of $Pd_2$, $Pd_3$ ($D_{3h}$) and $Pd_4$ ($C_{3v}$) Clusters in the Lowest Singlet Electronic States and $H_2$ Molecule**

| basis set for Pd | | basis I | basis II | reference |
|---|---|---|---|---|
| $Pd_2$ | $a$ | 2.762 | 2.743 | 2.87[d] |
| $Pd_3$ | $a$ | 2.515 | 2.832 | 2.92[e] |
| | $r$ | 1.452 | 1.635 | |
| $Pd_4$ | $a$ | 2.652 | 2.905 | 2.686;[a] 2.832[b] |
| | $r$ | 1.531 | 1.677 | |
| | $h$ | 2.165 | 2.371 | |
| $H_2$ | $d$ | 0.7615 | | 0.7461[c] |
| | $D$ | 107.4 | | 104.2[c] |

*Notations: $a$ and $d$ stand here for Pd−Pd and H−H bond lengths, respectively; $r$ is the distance from Pd atom to the center of $Pd_3$ triangle; $h$ is the height of $Pd_4$ pyramid. Distances $a$, $h$, $d$, and $r$ in Å, dissociation energy $D$ in kcal/mol. [a] MRSDCI calculations.[28] [b] CASSCF calculations.[28] [c] Experiment.[30] [d] MRSDCI calculations.[29] [e] MRSDCI calculations.[31]

and is included in the dissociation energies presented in Table 1. According to our estimations, LANL1DZ basis set is characterized by the minimal BSSE (−0.5 kcal/mol for PdH and near 0 for $Pd_2$), for basis I the BSSE is slightly bigger (−0.7 and −3 kcal/mol, respectively), and for basis II the BSSE is relatively large (−4 and −8 kcal/mol, respectively). Except for Table 1, energetic results presented in this work do not include BSSE corrections.

Although bare clusters are biradicals in the ground state, for stable hydrogenated clusters with dissociated H−H bonds the singlet state was found to be the most stable. Thus, in the present study we present the analysis of the PES cross-sections for the lowest multiplet state. The binding energy in the stationary points is determined as $E_b = E(Pd_n) + E(H_2) − E(Pd_nH_2)$ with respect to the minimal energy singlet states of palladium clusters.

**Results and Discussion**

**1. Individual Reactants**. The reference geometries obtained in our B3LYP calculations for the individual singlet $Pd_2$, $Pd_3$ ($D_{3h}$ symmetry), and $Pd_4$ ($C_{3v}$ symmetry) clusters (not the ground state) are listed in Table 2. For $Pd_2$ both basis sets used provide about the same interatomic distance while for the larger clusters the more extended basis gives Pd−Pd bond lengths by about 0.3 Å shorter. The optimized structure of the palladium tetramer is close to regular tetrahedron in both the basis sets.

Several sophisticated HF and DFT calculations of these clusters provide a broad range of data. Our B3LYP/LANL2DZ results agree well with the literature data[14,20] obtained at the same level of theory. Balasubramanian's MRSDCI calculations[26,28,31] (presented in Table 2) show slightly shorter Pd−Pd distances. The difference between B3LYP/LANL2DZ and MRSDCI results decreases with increase of cluster size.

For the $H_2$ molecule (Table 2) the dissociation energy is overestimated by 3% and bond length by ∼0.015 Å as compared to the corresponding experimental values.

**2. Pd−$H_2$ Interaction**. Since hydrogen interaction with palladium atom is well documented in literature, we present here the results of our calculations in order to trace the size dependencies in $Pd_n$−$H_2$ interactions. As was shown earlier,[4,7,9,11,12] in the Pd−$H_2$ system both side-on and end-on approach modes lead to the formation of weak complexes (Figure 1). For the most stable side-on structure (Figure 1a), B3LYP/LANL2DZ calculations provide a Pd−H bond of 1.683 Å and a H−Pd−H angle of 30.4°, in good agreement with MRSDCI results[7] (1.67 Å and 30°, respectively). Basis II yields the binding energy by 3 kcal/mol smaller and the optimized geometry more consistent with CASSCF results.[7] The second minimum, which corresponds to the dissociation of the H−H bond (Figure 1b), may be localized only with more extensive basis set, as in the case of classical HF calculations.[7] It lies 4.5 kcal/mol higher and has a Pd−H bond of 1.52 Å and a H−Pd−H angle of 69.8° in comparison with MRSDCI results[7] of 5.79 kcal/mol, 1.50 Å, and 62.0°, respectively. The linear H−Pd−H state (Figure 1c) has a considerably higher energy (by 53.2 and 48.3[7] kcal/mol at B3LYP/LANL2DZ and MRSDCI levels of theory, respectively) with notably longer Pd−H bonds (1.64 and 1.62[7] Å). At both the basis sets used, this complex is extremely unstable with respect to $H_2$ abstraction.

The end-on approach mode forms a very weakly bonded coordination structure (Figure 1d). The linear Pd−H−H complex with an unrelaxed $H_2$ molecule calculated at post-HF level with relativistic ECP[4] shows about the same Pd−H distance and stabilization energy of about 5.5 kcal/mol. The smaller basis set yields a slightly stronger connection for this complex.
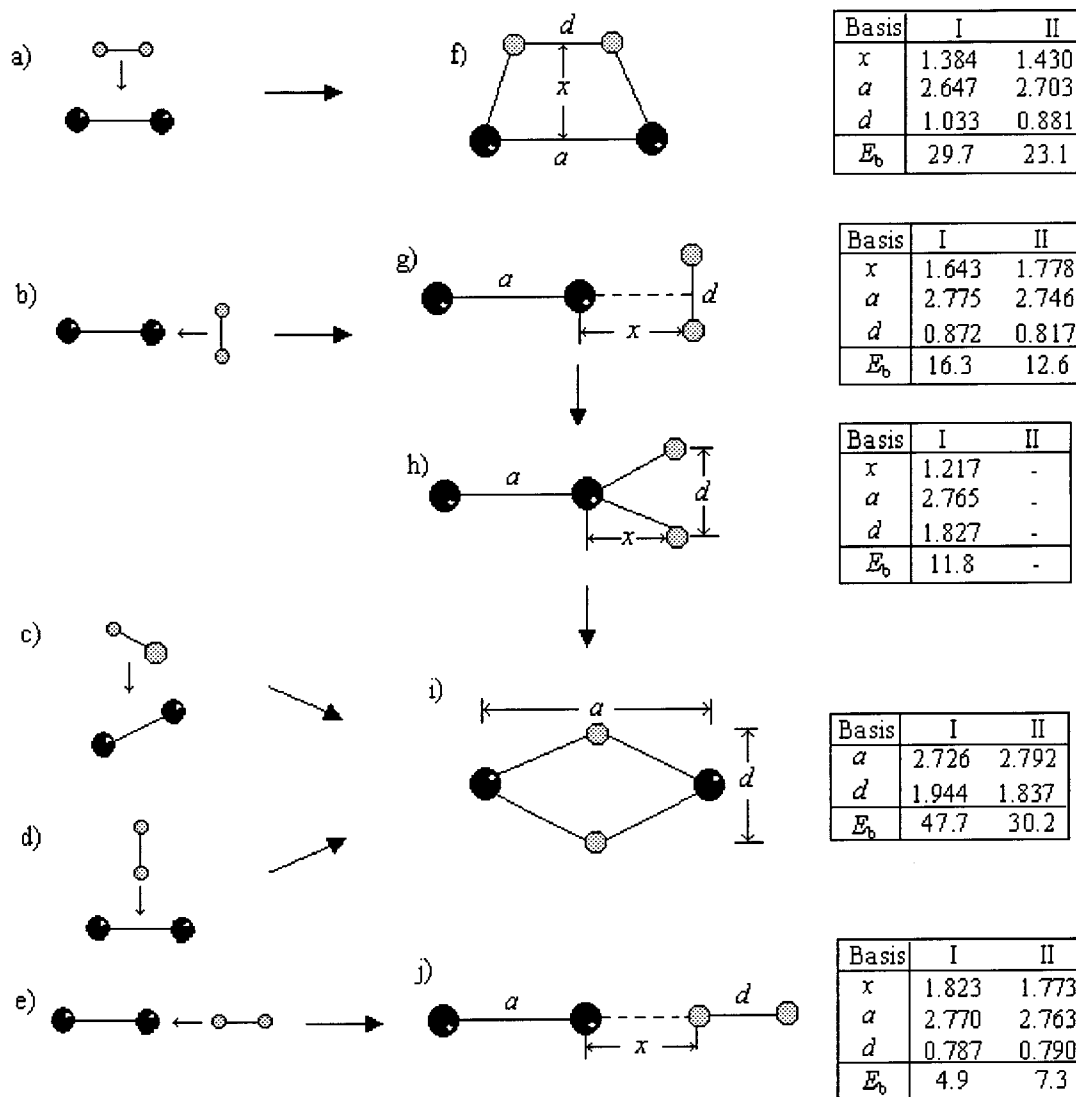
| Basis | I | II |
|---|---|---|
| $x$ | 1.384 | 1.430 |
| $a$ | 2.647 | 2.703 |
| $d$ | 1.033 | 0.881 |
| $E_b$ | 29.7 | 23.1 |

| Basis | I | II |
|---|---|---|
| $x$ | 1.643 | 1.778 |
| $a$ | 2.775 | 2.746 |
| $d$ | 0.872 | 0.817 |
| $E_b$ | 16.3 | 12.6 |

| Basis | I | II |
|---|---|---|
| $x$ | 1.217 | - |
| $a$ | 2.765 | - |
| $d$ | 1.827 | - |
| $E_b$ | 11.8 | - |

| Basis | I | II |
|---|---|---|
| $a$ | 2.726 | 2.792 |
| $d$ | 1.944 | 1.837 |
| $E_b$ | 47.7 | 30.2 |

| Basis | I | II |
|---|---|---|
| $x$ | 1.823 | 1.773 |
| $a$ | 2.770 | 2.763 |
| $d$ | 0.787 | 0.790 |
| $E_b$ | 4.9 | 7.3 |

**Figure 2.** Considered approach modes, structures, and corresponding binding energies of stationary states in the Pd$_2$–H$_2$ system.

**3. Pd$_2$–H$_2$ Interaction**. Five considered approach modes between hydrogen molecule and Pd$_2$ cluster are shown in Figure 2a–e. In the case of the parallel approach of reactants (Figure 2a) a planar trapezoidal complex (Figure 2f) is formed. Somewhat higher binding energy and a fairly longer H–H interatomic distance as compared to the most stable PdH$_2$ complex characterize this structure, but H-atoms still remain to be significantly bonded. The Mulliken population analysis reveals Pd–H bond occupation of 0.22 and 0.14 and H–H bond occupation of 0.102 and 0.150 in basis sets I and II, respectively. According to ref 9, the similar approach mode on Pt$_2$ leads to complete dissociation of the H–H bond and the resulting complex undergoes transformation to nonplanar structure with a H–Pt–Pt–H dihedral angle of 106.4°, which presents the ground state of the system. This difference is explained by the analysis of electronic structures of palladium and platinum dimers presented in ref 9.

The perpendicular Pd$_2$ bisecting H$_2$ approach (Figure 2b) captures hydrogen in two weak complexes (Figure 2g,h) similar to those formed by a single Pd atom (Figure 1a,b). Again, the second state (with dissociated H–H bond) is less stable than the first one (with H–H bond length softly relaxed) and may not be localized with basis II. Moving further along the approach mode, these complexes transform to the most stable planar

rhomboid Pd$_2$H$_2$ structure (Figure 2i). This last structure is formed as well in the cases of perpendicular side-on (Figure 2c) and end-on (Figure 2d) approaches of the hydrogen molecule toward the center of the Pd–Pd bond. The H–H bond is strongly dissociated in this structure. Despite the close geometric parameters, the binding energies obtained for this configuration with the two basis sets differ significantly. As in ref 9, the nonplanar structure with the H–H bond being 0.093 Å above Pd–Pd bond, which have the same binding energy and about the same interatomic distances, may be identified using basis I.

The end-on approach of a hydrogen molecule toward one of the Pd atoms ($C_{\infty v}$ symmetry, Figure 2e) leads to a significantly weaker complex (Figure 2j) with much less activated H–H bond as compared to the corresponding structure in the Pd–H$_2$ system (Figure 1d) in both basis sets.

Presented geometric results are in a close agreement with those of refs 3,5,12 while the binding energies are significantly lower. In the recent MCSCF calculations with the relativistic ECP,[3] the binding energies were found to be 37.0, 22.0, and 65 kcal/mol for the structures presented in Figure 2f,g,i, respectively. The weak coordination of the H$_2$ molecule was obtained in this work for the end-on H$_2$ approach bisecting Pd$_2$ bond (Figure 2d). Probably, fixing of the Pd–Pd bond length hampers H$_2$ dissociation in this case. Both geometry and binding energy

for the most stable structure (Figure 2i) agree well with the DFT results[9] ($E_b$ = 45.9 kcal/mol with respect to the singlet $Pd_2$).

**4. $Pd_3-H_2$ Interaction.** The end-on $H_2$ approaching the $Pd_3$ cluster along $C_{3v}$ axis (Figure 3a), as well as $H_2$ approaching the base of the $Pd_3$ triangle along the $C_{2v}$ axis in a side-on perpendicular way (Figure 3b), leads to the formation of a fairly stable $Pd_3H_2$ complex displayed in Figure 3h. In basis II this is the most stable configuration. In this state two H-atoms are situated symmetrically relative to the $Pd_3$ plane at a distance of 1.6−1.8 Å, i.e., the hydrogen molecule is dissociated. As compared to the bare cluster, Pd−Pd distances increase from 2.515 to 2.725 Å in basis I and decrease from 2.832 to 2.751 Å in basis II. Both the basis sets yield similar binding energies, which again are significantly lower than those obtained in the MCSCF calculations[3] for the fixed geometry of the metal cluster with the optimized H−H distance of 1.4 Å (55 kcal/mol).

The side-on approach of a hydrogen molecule toward the triangle vertex in the perpendicular plane (Figure 3c) forms first the van der Waals complex (Figure 3i) separated by an activation barrier from the stable structure with dissociated hydrogen molecule presented in Figure 3h. The MCSCF calculations[3] showed this complex to have about the same geometry and significantly higher stabilization energy (23.7 kcal/mol).

The end-on $H_2$ approach toward the $Pd_3$ triangle vertex along $C_{2v}$ axis (Figure 3d) forms a very weak coordination complex (Figure 3j) with soft relaxation of the geometry of both reactants. As in case of the similar $Pd_2-H_2$ complex (Figure 2i), basis II overestimates the binding energy.

Two considered in-plane approach modes (Figure 3e,f) perform a hydrogen capture in molecular forms shown in Figure 3k,l, the later of which may be localized only with basis I. These complexes further transform to the stable planar structure involving two hydrogen atoms connected to the Pd−Pd bonds (Figure 3m). All these three minima were obtained in the CASSCF−MRSDCI calculations with optimization of Pd−Pd bond lengths under the $C_{3v}$ symmetry constraint[8] with last of them considered as the ground state of $Pd_3H_2$ complex. The MCSCF calculations with fixed cluster geometry[3] did not show the second minimum.

For the complex in Figure 3k the binding energies are −10.5, +23.9, and +0.9 kcal/mol with the optimized $Pd_3-H_2$ distances ($x$) of 1.99, 1.5, and 2.52 Å and H−H bond length ($d$) of 0.81, 0.9, and 0.766 Å at the MRSDCI,[8] MCSCF,[3] and B3LYP/LANL2DZ levels of theory, respectively. For the complex in Figure 3l our B3LYP binding energy $E_b$ = 13.8 kcal/mol is very close to that of 16.5 kcal/mol obtained in the MRSDCI calculations;[8] however, the optimized geometry differs significantly. Three Pd−Pd bonds of 2.85 Å, $d_{Pd-H}$ = 1.47, $d_{H-H}$ = 1.11, and $x$ = 2.01 Å were found in ref 8. Allowing optimization of the geometry under $C_{2v}$ symmetry constraints shows the notable deviation of $Pd_3$ cluster from the regular triangle. We obtained two Pd−Pd bonds of 2.662 and one of 3.004 Å that lead to shorter capture distance ($x$ = 1.221 Å) and slightly weaker $Pd_3-H_2$ interaction: $d_{Pd-H}$ = 1.583, $d_{H-H}$ = 0.988 Å. The effect of proper optimization of the geometry is even more pronounced for the last structure (Figure 3m). In this case we obtained two side Pd−Pd bonds of 2.976 Å, the base of triangle of 2.641 Å, and H-atoms being slightly shifted from the center of the Pd−Pd bond toward the base ($d_{Pd-H}$ = 1.598 and 1.663 Å) in comparison with three Pd−Pd distances of 2.99 Å and four Pd−H distances of 1.57 Å from ref 8. As a result, the stabilization energy obtained in our calculations (40.0 kcal/mol) is much higher than that of ref 8 (20.3 kcal/mol). The MCSCF

calculations[3] provide $E_b$ = 55.9 kcal/mol for the only stable configuration obtained for the considered approach mode (Figure 3m), but this minimum corresponds to hydrogen molecule with $d_{H-H}$ = 0.96 Å located inside the $Pd_3$ cluster with frozen geometry of the bulk metal. Thus, it may be seen that optimization of the geometry of small palladium clusters is of paramount importance for the correct description of their interactions with hydrogen. The MCSCF results[3] significantly overestimated binding energies for all considered complexes and do not show minima for some of weakly bonded structures.
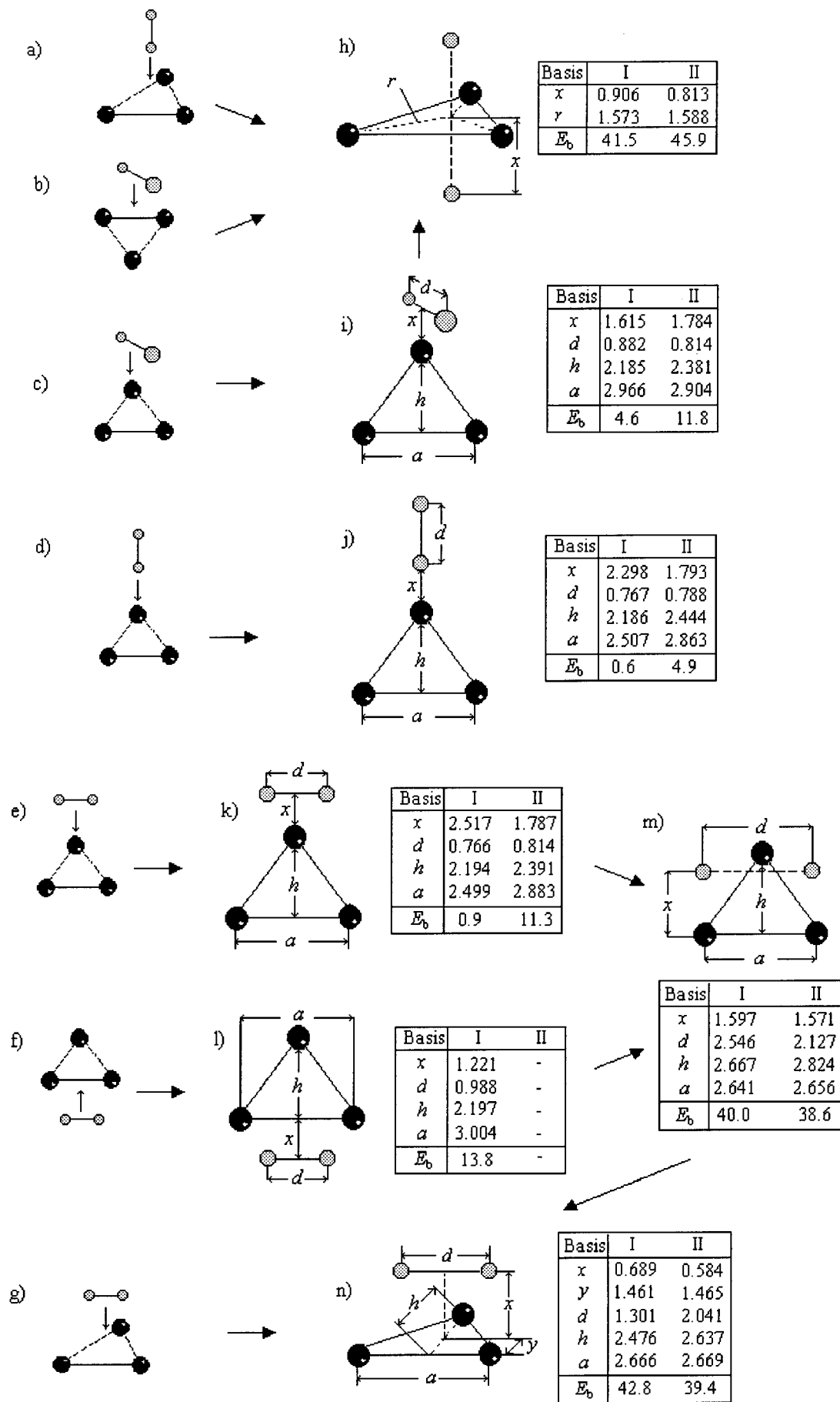
The most stable $Pd_3H_2$ configuration at B3LYP/LANL2DZ level of theory corresponds to two hydrogen atoms sitting on Pd−Pd bonds out of the $Pd_3$ plane (Figure 3n). This configuration might be obtained by transformation of the planar structure shown in Figure 3m, as well as by spontaneous hydrogen dissociation via the out-of-plane approach mode shown in Figure 3g. The geometry of the complex is very close to that presented in ref 10, but the binding energy is by 7.8 kcal/mol higher as compared to their results.

**5. $Pd_4-H_2$ Interaction.** In this system the stationary states were localized for six directions of $H_2$ approach modes toward $Pd_4$ clusters under the $C_{3v}$ (Figure 4a,b), $C_{2v}$ (Figure 4c−e), and $C_s$ (Figure 4f) symmetry constraints. In basis I the end-on $H_2$ to top $Pd_4$ direction (Figure 4a) leads to the formation of a very weak complex ($E_b$ = 1.7 kcal/mol) with a Pd−H bond of 2.04 Å and H−H bond expansion by 1.8% with respect to free $H_2$ molecule (Figure 4g). Basis II yields the deeper minimum (6.4 kcal/mol) at a Pd−H distance of 1.79 Å and 3.3% elongation of the H−H bond. In both basis sets this stable state may be assigned to a physical adsorption.

The end-on approach way toward the base of the pyramid along $C_{3v}$ axis (Figure 4b) provides a structure in which a dihydrogen molecule is significantly dissociated ($d_{H-H} \sim$ 1.6−1.7 Å, Figure 4h). In this state one of the H atoms is situated inside the cluster and another one occupies the 3-fold outer position. The structure of $Pd_4$ core in this complex is significantly perturbed as compared to the bare cluster: in basis I all interatomic distances increase, while in basis II the cluster contracts around and elongates along the $C_{3v}$ symmetry axis. Although the configurations obtained in terms of both basis sets are close to each other, they differ considerably in the binding energy (by ∼26 kcal/mol).

The local minimum shown in Figure 4i is formed in a side-on dihydrogen approach direction toward the Pd−Pd bond in both parallel and perpendicular modes (Figure 4c,d). This state may be interpreted as a dissociative adsorption: each of the H atoms is bound to three Pd atoms of the tetramer faces, and the H−H distance is about 2 Å. Again, the geometrical structures of this stable state as calculated with basis sets I and II are very close, and the binding energy in basis I is lower than that in basis II by about 20 kcal/mol. Basis II yields this structure as the ground state of the $Pd_4H_2$ complex. The weakly bonded state determined in basis I for the parallel approach mode in the $Pd_3-H_2$ system may not be localized here, probably due to the slightly longer Pd−Pd distance and to easier cluster relaxation allowing the hydrogen molecule to pass through the Pd−Pd bond without an activation barrier.

The end-on $H_2$ attack to the Pd−Pd bond directed along the $C_{2v}$ symmetry axis (Figure 4e) results in complete dissociation of a dihydrogen molecule. In the stable state formed (Figure 4j) H-atoms are bonded to the parallel Pd−Pd bond and $d_{H-H}$ = 3.4−3.5 Å depending on the basis set. In this state the structure of the $Pd_4$ skeleton is noticeably perturbed as compared to the bare cluster. The binding energy for this state is close to

a)

b)

c)

d)

e)

f)

g)

h)

| Basis | I | II |
|-------|-------|-------|
| $x$ | 0.906 | 0.813 |
| $r$ | 1.573 | 1.588 |
| $E_b$ | 41.5 | 45.9 |

i)

| Basis | I | II |
|-------|-------|-------|
| $x$ | 1.615 | 1.784 |
| $d$ | 0.882 | 0.814 |
| $h$ | 2.185 | 2.381 |
| $a$ | 2.966 | 2.904 |
| $E_b$ | 4.6 | 11.8 |

j)

| Basis | I | II |
|-------|-------|-------|
| $x$ | 2.298 | 1.793 |
| $d$ | 0.767 | 0.788 |
| $h$ | 2.186 | 2.444 |
| $a$ | 2.507 | 2.863 |
| $E_b$ | 0.6 | 4.9 |

k)

| Basis | I | II |
|-------|-------|-------|
| $x$ | 2.517 | 1.787 |
| $d$ | 0.766 | 0.814 |
| $h$ | 2.194 | 2.391 |
| $a$ | 2.499 | 2.883 |
| $E_b$ | 0.9 | 11.3 |

m)

| Basis | I | II |
|-------|-------|-------|
| $x$ | 1.597 | 1.571 |
| $d$ | 2.546 | 2.127 |
| $h$ | 2.667 | 2.824 |
| $a$ | 2.641 | 2.656 |
| $E_b$ | 40.0 | 38.6 |

l)

| Basis | I | II |
|-------|-------|-------|
| $x$ | 1.221 | - |
| $d$ | 0.988 | - |
| $h$ | 2.197 | - |
| $a$ | 3.004 | - |
| $E_b$ | 13.8 | - |

n)

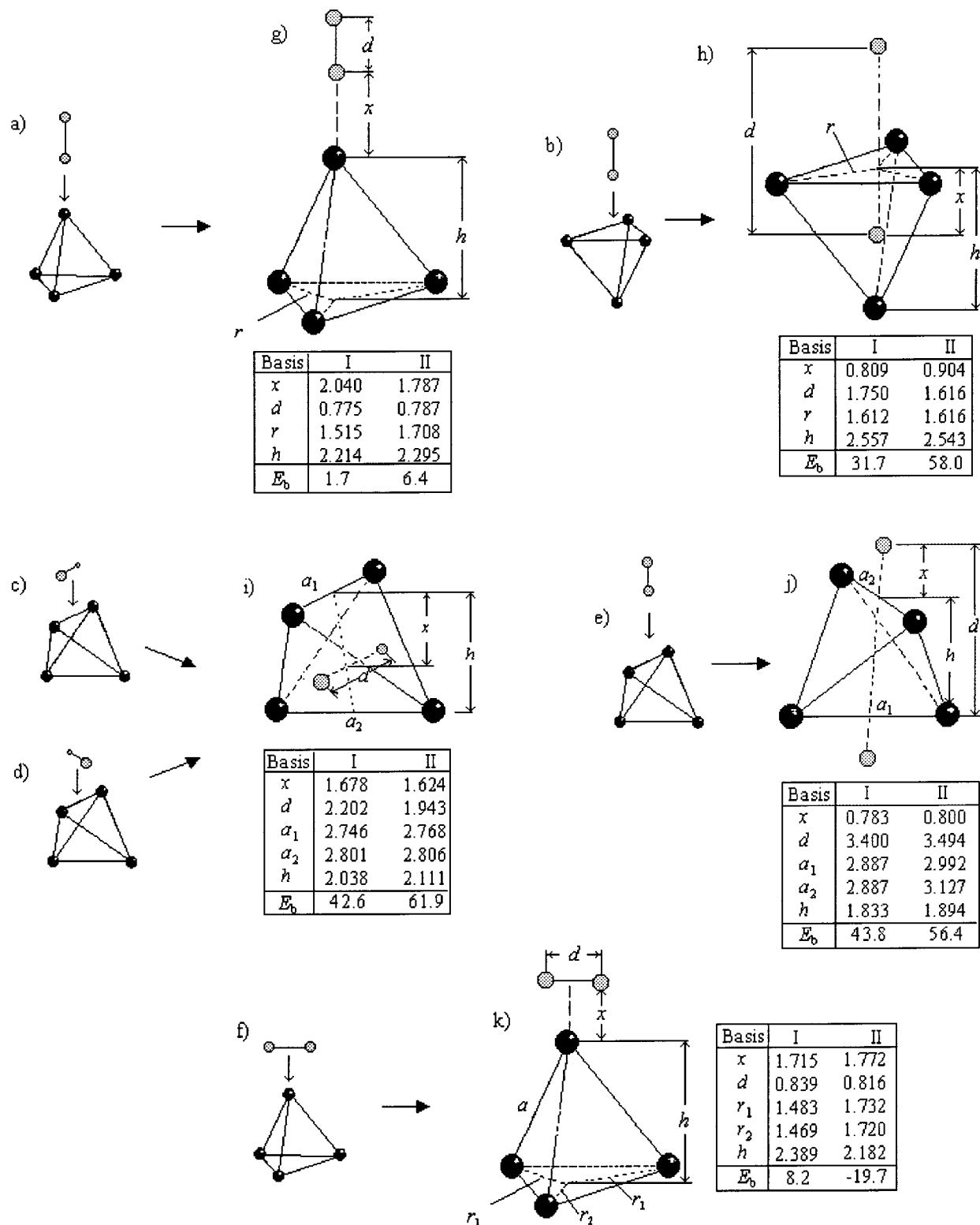| Basis | I | II |
|-------|-------|-------|
| $x$ | 0.689 | 0.584 |
| $y$ | 1.461 | 1.465 |
| $d$ | 1.301 | 2.041 |
| $h$ | 2.476 | 2.637 |
| $a$ | 2.666 | 2.669 |
| $E_b$ | 42.8 | 39.4 |

**Figure 3.** Considered approach modes, structures, and corresponding binding energies of stationary states in the Pd$_3$−H$_2$ system.

| Basis | I | II |
|---|---|---|
| $x$ | 2.040 | 1.787 |
| $d$ | 0.775 | 0.787 |
| $r$ | 1.515 | 1.708 |
| $h$ | 2.214 | 2.295 |
| $E_b$ | 1.7 | 6.4 |

| Basis | I | II |
|---|---|---|
| $x$ | 0.809 | 0.904 |
| $d$ | 1.750 | 1.616 |
| $r$ | 1.612 | 1.616 |
| $h$ | 2.557 | 2.543 |
| $E_b$ | 31.7 | 58.0 |

| Basis | I | II |
|---|---|---|
| $x$ | 1.678 | 1.624 |
| $d$ | 2.202 | 1.943 |
| $a_1$ | 2.746 | 2.768 |
| $a_2$ | 2.801 | 2.806 |
| $h$ | 2.038 | 2.111 |
| $E_b$ | 42.6 | 61.9 |

| Basis | I | II |
|---|---|---|
| $x$ | 0.783 | 0.800 |
| $d$ | 3.400 | 3.494 |
| $a_1$ | 2.887 | 2.992 |
| $a_2$ | 2.887 | 3.127 |
| $h$ | 1.833 | 1.894 |
| $E_b$ | 43.8 | 56.4 |

| Basis | I | II |
|---|---|---|
| $x$ | 1.715 | 1.772 |
| $d$ | 0.839 | 0.816 |
| $r_1$ | 1.483 | 1.732 |
| $r_2$ | 1.469 | 1.720 |
| $h$ | 2.389 | 2.182 |
| $E_b$ | 8.2 | -19.7 |

**Figure 4.** Considered approach modes, structures, and corresponding binding energies of stationary states in the $Pd_3-H_2$ system.

that obtained for two H-atoms in 3-fold positions. This structure is a candidate for the global minimum of the system in the extended basis set.

The last approach mode we discuss here is the side-on $H_2$ direction toward the top of the $Pd_4$ pyramid (Figure 4f). The molecular adsorption state (Figure 4k) was found to precede the dissociation. This state is unstable with respect to $H_2$ desorption with basis I. The structure of the corresponding stable state is the same as presented in Figure 4i.

## 6. Discussion

Few local minima found in each of $Pd_n-H_2$ ($n = 1-4$) system coincide with different degrees of hydrogen activation by palladium. A state of the molecular adsorption with the binding energy of several kilocalories per mole is characterized by soft relaxation of reactants' geometry. This state may be assigned to physical adsorption. It was localized for end-on and side-on hydrogen approach modes toward one of the metal atoms in
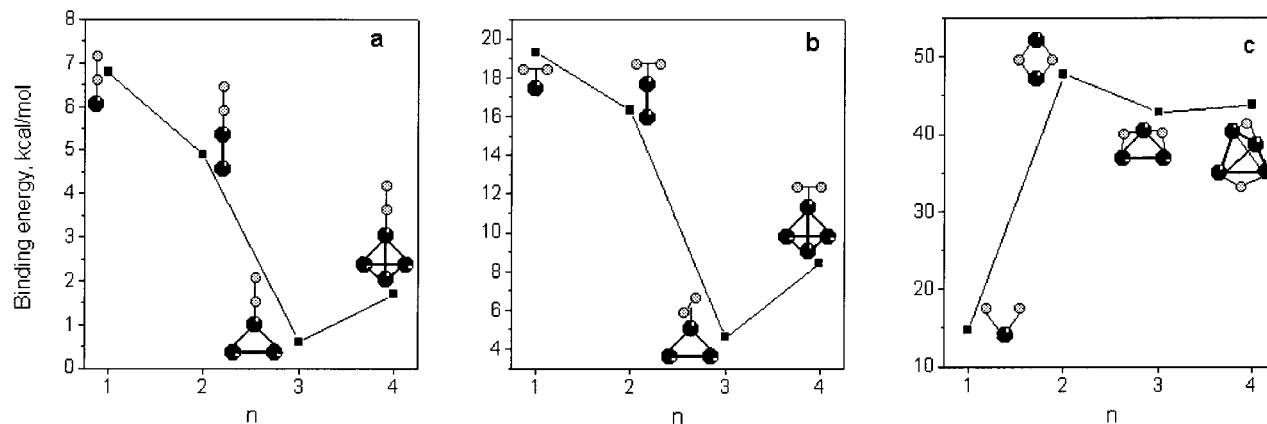
Interactions of Dihydrogen and Pd$_n$ ($n = 1-4$) Clusters

*J. Phys. Chem. A, Vol. 104, No. 34, 2000* **8095**



**Figure 5.** Size dependencies of the binding energy obtained in B3LYP/LANL2DZ calculations for the molecular end-on (a) and side-on (b) and for the most stable dissociative (c) hydrogen coordination.

Pd$_n$ clusters. In both cases the characteristic Pd$_n$–H$_2$ distance tends to increase with increase of cluster size, with consequent weakening of intermolecular interaction and stabilization energy. Figure 5a,b shows the size dependence of binding energy for the molecular end-on and side-on hydrogen bonding to palladium atom (in the most stable configuration if more than one exist).

Molecular complexes similar to those we obtained for side-on to Pd atom approach mode were localized by Dong and Hafner[32] in GGA slab calculations of hydrogen activation on bulk Pd (111) surface at coverage $\theta = 2/3$. Both the geometry of surface Pd–H$_2$ complexes ($d_{H-H} = 0.82-0.84$ Å, adsorption height $x = 1.74-1.80$ Å) and the adsorption energy (4.8–5.3 kcal/mol) obtained in this work are very close to those we found for Pd$_3$ and Pd$_4$ clusters. Such complexes with weakly bonded activated dihydrogen might play an important role in catalytic interactions.

The dissociative adsorption state is not stable for hydrogen interaction with a single palladium atom. Pd$_2$ cluster forms very stable dissociative structure in both side-on and end-on H$_2$ approach modes toward a Pd–Pd bond. The nonplanar complex with two hydrogen atoms in the bridge positions corresponds to the ground state in the Pd$_3$–H$_2$ system; however, the Pd$_3$H$_2$ complex with hydrogen atoms on the $C_{3v}$ axis of Pd$_3$ cluster forming a double 3-fold site is located only 1.3 kcal/mol over the ground state. Similarly, 2-fold coordination appears to be the most stable for the palladium tetramer. The binding energy of the 3-fold coordination is smaller by 1.2 kcal/mol for this cluster. The third local minimum in the Pd–H$_2$ system is located 12.2 kcal/mol over the ground state and corresponds to the dissociated H$_2$ molecule sitting on the $C_{3v}$ axis with one of the H atoms inside the Pd$_4$ tetramer and another one in the outside 3-fold position. Figure 5c displays the binding energy of the most stable dissociative structure as a function of cluster size. Presented dependence qualitatively agrees with the experimentally observed size dependence of the reactivity of small palladium clusters.[2]

These results differ significantly from those for bulk Pd (111) surface, for which both experimental[33] and theoretical[32] data indicate that 3-fold positions are more stable than 2-fold ones. The adsorption energy for the most stable 3-fold coordination on Pd (111) surface of 20.9 kcal/mol[32] (22.9 kcal/mol[33]) is much smaller than that we obtained for Pd$_3$ and Pd$_4$ clusters (41.5 and 42.6 kcal/mol, respectively). In contrast to Pd$_{2-4}$ clusters, the perpendicular side-on hydrogen approach toward the center of the Pd–Pd bond on the surface is an activated dissociation pathway and leads to a relatively weakly bonded structure

($E_b = 15$ kcal/mol) with two hydrogen atoms in nearest-neighboring 3-fold positions.[32] It might be important to note here that the substrate structure was frozen at the bulk *fcc* lattice in this work. The dissociative Pd$_4$H$_2$ structure with one of the hydrogen atoms sitting inside the cluster and another one being localized in an outside 3-fold position, which appears quite stable in our calculations, was not considered for the bulk surface.

The state of intermediate hydrogen activation with H–H bond parallel to Pd–Pd bond is fairly stable for Pd$_2$ cluster and may be localized in the Pd$_3$–H$_2$ system, while in the Pd$_4$–H$_2$ system a hydrogen molecule passes through the Pd–Pd bond and dissociates without an activation barrier. In the case of the Pd (111) surface, this reaction pathway leads to an end-configuration unstable with respect to the noninteracting H$_2$ and palladium.

The significant differences in hydrogen activation on bulk palladium surfaces and small clusters might underlay their different catalytic behavior in reactions of hydrogenation.

## Conclusions

The interaction of a dihydrogen with Pd$_n$ clusters ($n = 1-4$) was studied by hybrid DFT method with two basis sets and with optimization of the geometry under given symmetry constraint. As was shown earlier for traditional ab initio methods, the extended basis set is very important even for the qualitative description of the Pd$_n$–H$_2$ system. The relativistic ECP LANL2DZ basis shows a good agreement with the CASSCF–MRSDCI results for the equivalent calculations. The proper optimization of the geometry, which is significantly less expansive in the framework of DFT approach, appears to be extremely important at least for some of the considered configurations.

As in case of bulk Pd (111) surface, in Pd$_n$–H$_2$ ($n = 1-4$) systems some of reaction pathways lead to nonactivated hydrogen dissociation. For several approach modes, a precursor state precedes the dissociation. The geometry and binding energy of weakly bonded complexes with softly relaxed hydrogen molecule coordinated on one palladium atom are very close for Pd$_{3-4}$ clusters and Pd (111) surface. The size dependence of the most stable Pd$_n$H$_2$ complexes qualitatively agrees with the experimentally observed reactivity of small palladium clusters,[2] i.e., the palladium dimer was found to form the most stable dihydrogenated complex. In contrast to the bulk surface, 2- and 3-fold coordination positions exhibit very close stability of hydrogen bonding in Pd$_3$ and Pd$_4$ clusters with the former position slightly more stable than the latter one. Comparing with

**8096** *J. Phys. Chem. A, Vol. 104, No. 34, 2000*

Efremenko et al.

the bulk surface, in the case of small palladium clusters the binding energy for the most stable configuration is significantly higher.

## References and Notes

(1) Che, M.; Bennett, C. O. *Adv. Catal.* **1989**, *36*, 55.

(2) Fayet, P.; Kaldor, A.; Cox, D. M. *J. Chem. Phys.* **1990**, *92*, 254.

(3) Castillo, S.; Cruz, A.; Bertin, V.; Poulain, E.; Arellano, J. S.; Del Angel, G. *Int. J. Quantum Chem.* **1997**, *62*, 29.

(4) Novaro, O.; Jarque, C. *Theor. Chim. Acta* **1991**, *80*, 19.

(5) Nakatsuji, H.; Hada, M.; Yonezawa, T. *J. Am. Chem. Soc.* **1987**, *109*, 1902; Nakatsuji, H.; Hada, M. *J. Am. Chem. Soc.* **1985**, *107*, 8264.

(6) Bagatur'yants, A. A.; Anikin, N. A.; Zhidomirov, G. M.; Kazanskii, V. B. *Russ. J. Phys. Chem.* **1981**, *55*, 1157.

(7) Balasubramanian, K.; Feng, P. Y.; Liao, M. Z. *J. Chem. Phys.* **1988**, *88*, 6955.

(8) Dai, D.; Liao, D. W.; Balasubramanian, K. *J. Chem. Phys.* **1995**, *102*, 7530.

(9) Cui, Q.; Musaev, D. G.; Morokuma, K. *J. Chem. Phys.* **1998**, *108*, 8418.

(10) Cui, Q.; Musaev, D. G.; Morokuma, K. *J. Phys. Chem.* **1998**, *102*, 6373.

(11) Siegbahn, P. E. M. *Theor. Chim. Acta* **1994**, *87*, 441.

(12) Louis, E.; Moscardo, F.; San-Fabian, E.; Perez-Jorda, J. M. *Phys. Rev. B* **1990**, *42*, 42.

(13) Efremenko, I.; Sheintuch, M. *Surf. Sci.* **1998**, *414*, 148.

(14) Valerio, G.; Toulhoat, H. *J. Phys. Chem.* **1996**, *100*, 10827.

(15) Frisch, M. J.; Trucks, G. W.; Schlegel, H. B.; Gill, P. M. W.; Johnson, B. G.; Robb, M. A.; Cheeseman, J. R.; Keith, T. A.; Peterson, G. A.; Montgomery, J. H.; Raghavachari, K.; Al-Laham, M. A.; Zakrewski, V. G.; Ortiz, J. V.; Foresman, J. B.; Cioslowski, J.; Stefanov, B. B.; Nanayakhara, A.; Challacombe, M.; Peng, C. Y.; Ayala, P. Y.; Chen, W.; Wong, M. W.; Andres, J. L.; Replogle, E. S.; Gomperts, R.; Martin, R. L.; Fox, D. J.; Binkley, J. S.; Defrees, D. J.; Baker, J.; Stewart, J. P.; Head-Gordon, M.; Gonzales, C.; Pople, J. A. *Gaussian 94*; Gaussian, Inc., Pittsburgh, PA, 1995.

(16) Becke, A. D. *J. Chem. Phys.* **1993**, *98*, 5648.

(17) Lee, C.; Yang, W.; Parr, R. G. *Phys. Rev. B* **1988**, *37*, 785.

(18) Woon, D. E.; Dunning, T. H., Jr. *J. Chem. Phys.* **1993**, *98*, 1358.

(19) Hay, P. J.; Wadt, W. R. *J. Chem. Phys.* **1985**, *82*, 270; Hay, P. J.; Wadt, W. R. *J. Chem. Phys.* **1985**, *82*, 299.

(20) Zacarias, A. G.; Castro, M.; Tour, J. M.; Seminario, J. M. *J. Phys. Chem. A* **1999**, *103*, 7692.

(21) Akinaga, Y.; Takesugu, T.; Hirao, K. *J. Chem. Phys.* **1998**, *109*, 11010.

(22) Knight, L. B.; Weltner, W. *J. Mol. Spectrosc.* **1971**, *40*, 317.

(23) Huber, K. P.; Herzberg, G. *Molecular Spectra and Molecular Structures, 4: Constants of Diatomic Molecules*; Van Nostrand Reinhold: New York, 1979.

(24) Tolbert, M. A.; Beauchamp, J. L. *J. Phys. Chem.* **1986**, *90*, 5015.

(25) Lin, S.; Strauss, S.; Kant, A. *J. Chem. Phys.* **1969**, *51*, 2282.

(26) Ho, J.; Ervin, K. M.; Polak, M. L.; Gilles, M. K.; Lineberger, W. C. *J. Chem. Phys.* **1991**, *95*, 4845.

(27) Boys, S. B.; Bernardi, F. *Mol. Phys.* **1970**, 19, 553.

(28) Dai, D.; Balasubramanian, K. *J. Chem. Phys.* **1995**, *103*, 648.

(29) Balasubramanian, K. *J. Chem. Phys.* **1988**, *89*, 6310.

(30) Weast, R. C.; Selby, S. M. *Handbook of Chemistry and Physics*, 55th ed.; Chemical Rubber Co.: Cleveland, OH, 1974.

(31) Balasubramanian, K. *J. Chem. Phys.* **1989**, *91*, 307.

(32) Dong, W.; Hafner, J. *Phys. Rev. B* **1997**, *56*, 15396.

(33) Conrad, H.; Ertl, G.; Latta, E. E. *Surf. Sci.* **1974**, *41*, 435.